ACS Sustainable Chemistry & Engineering

pubs.acs.org/journal/ascecg

Research Article

Artificial Fusion Protein to Facilitate Calcium Carbonate Mineralization on Insoluble Polysaccharide for Efficient Biocementation

Thiloththama H. K. Nawarathna, Kazunori Nakashima,* Tetsuya Kawabe, Wilson Mwandira, Kiyofumi Kurumisawa, and Satoru Kawasaki

Cite This: *ACS Sustainable Chem. Eng.* 2021, 9, 11493−11502

Read Online

ACCESS | Metrics & More | Article Recommendations | Supporting Information

ABSTRACT: Biomineralization is a process of mineral formation in living organisms. Compared with nonbiogenic minerals, biominerals can be defined as organic−inorganic hybrid materials that have excellent physical and optical properties. In the current study, an artificial protein mimicking the outer shell of crayfish, composed of $CaCO_3$, chitin, and proteins, was developed to facilitate organic−inorganic hybrid material formation by precipitation of calcium carbonate on the chitin matrix. The fusion protein (CaBP-ChBD) was constructed by introducing a short-sequence calcite-binding peptide (CaBP) into the chitin-binding domain (ChBD). Calcium carbonate precipitation experiments by enzymatic urea hydrolysis revealed that a significant increase in the $CaCO_3$ formation was achieved by adding CaBP-ChBD. Also, $CaCO_3$ was efficiently deposited on chitin particles decorated with CaBP-ChBD. Most interestingly, CaBP-ChBD would improve the performance in sand solidification more efficiently and sustainably in the process of biocementation technique. The developed recombinant protein could be used for the sustainable production of organic−inorganic green materials for engineering applications.

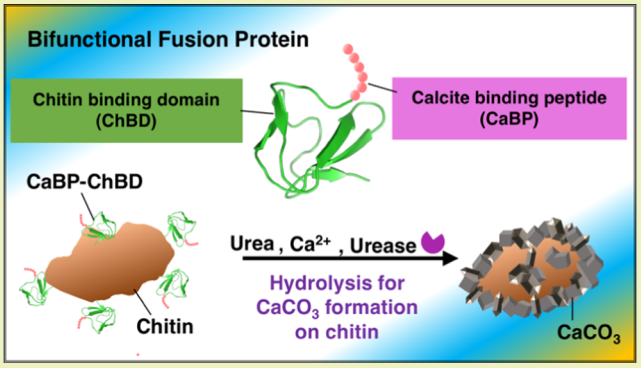

KEYWORDS: *recombinant protein, hybrid materials, biopolymer, calcium carbonate, biocementation*

INTRODUCTION

Biomineralization is a process of crystal nucleation and growth, and it is mostly controlled by organic macromolecules such as proteins, polypeptides, and polysaccharides.[1,2] Therefore, biominerals can be simply defined as organic−inorganic hybrid materials, and they are essential components in living organisms to support their different functions.[3,4] Compared with nonbiogenic minerals, biominerals are formed under mild conditions at near-neutral pH and ambient temperature, and they exhibit higher mechanical strength than nonbiogenic minerals.[3] Hydroxyapatite in the bones and teeth of mammals,[5] calcium carbonate in molluscan shells,[6] and amorphous silica in diatoms[7] and marine sponges[8] are well-known examples of biomineral formation.

Among the biominerals available in nature, most of them are calcium-bearing minerals, and calcium carbonate ($CaCO_3$) is the most dominant type of biomineral.[9] Coccoliths of coccolithophores, exoskeletons of crustaceans, and the nacre of mollusk shells mainly consist of biogenic $CaCO_3$ and exhibit excellent mechanical and optical properties.[9,10] For example, the strength of the nacre of a mollusk shell is 3000 times higher than that of pure $CaCO_3$.[11] Nacre has a brick-and-mortar structure, in which inorganic platelike aragonite $CaCO_3$ crystals (brick) are cemented with preorganized chitin sheets (mortar).[12] This structure provides the extensive mechanical strength of the nacre.

During the formation of biogenic $CaCO_3$, matrix proteins act as a template or starting point, and they play a vital role in the efficient formation of minerals on the organic matrix. To date, a number of proteins have been identified from the various species associated with the formation of $CaCO_3$ biominerals.[13−15] One of the best examples available in nature is the exoskeleton of the crayfish, in which $CaCO_3$ is deposited upon a chitin matrix with the assistance of the acidic protein CAP-1.[4,16] CAP-1 has a "Rebers−Riddiford" consensus sequence, and it helps the binding to the chitin. Also, this protein tends to be acidic owing to the associated seven acidic amino acids at the C-terminus, which facilitates $CaCO_3$ formation.[16,17] Similarly, chitin-binding type 2 domain (ChtBD2) has been identified

Received: June 3, 2021
Revised: August 2, 2021
Published: August 12, 2021

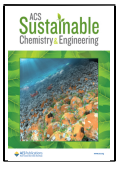

from the multifunctional matrix protein, hichin from the mantle of *H. cumingii*, which is involved in shell and pearl biomenralization.[18] The matrix protein PPP-10 in the periostracum of the pearl oyster has a chitin-binding ability and mainly supports the self-assembly of the periostracum.[19] Similarly, blue mussel shell protein 120 (BMSP-120) in the nacreous of the *Mytilus galloprovincialis* has peritrophin-A chitin-binding domain, which facilitates the nacreous layer formation,[20] and interlamellar matrix protein pearlin in nacreous layer of *Pinctada margaritifera* contributes to calcium and chitin binding in nacreous layer.[21]

In addition to the strength gain, biomacromolecules control the formation of minerals with nano-structural regularity and specific crystallographic phases, morphologies, and orientations,[15] which improve the fracture resistance and toughness of biogenic minerals, making them more feasible to use for certain industrial applications.[22]

By considering all of these factors, researchers have recently attempted to mimic the concept of biomineral formation in the synthesis of $CaCO_3$-organic hybrid materials for their associated excellent physical and optical properties. $CaCO_3$ biominerals can be extensively used in biomedical applications. Alternatively, the biological formation of $CaCO_3$ by enzyme-induced carbonate precipitation (EICP) has recently gained much attention as an efficient cementing material to solidify weak soils.[23−25]

EICP is a biogeochemical process catalyzed by urease.[26] Urease hydrolyzes urea to produce ammonia and bicarbonate ions. Bicarbonate ions instantaneously give $CaCO_3$ in the presence of Ca^{2+} ions under alkaline condition, which is induced by the generated ammonia. Formed $CaCO_3$ can act as a cementing material to bind sand particles, and this process or technique is called biocementation. In biocementation by EICP, effective filling of the pore spaces between sand particles with $CaCO_3$ is essential to get better strength and stiffness. $CaCO_3$ formation by the EICP process can be further increased by adding biomacromolecules such as xanthan gum, guar gum, poly (acrylic acid) (PAA), etc.[27,28] In this process, the efficient deposition of $CaCO_3$ on organic materials is essential to obtain desired strength.

To fulfill these expectations, the aim of this research was to develop a novel artificial fusion protein that could be directed toward efficient precipitation of $CaCO_3$ on chitin. Chitin was selected as an organic matrix because it is one of the most abundant, insoluble, linear polysaccharides available in nature, and it is mostly associated with $CaCO_3$ biomineralization.[12,16,29] The chitin-binding domain (ChBD) from chitinase was used as the chitin-binding site because it has a high binding affinity to chitin,[30−32] whereas a short sequence of calcite-binding peptide (CaBP) was used as the calcite-binding site.[33,34] The fusion protein had both a calcium-binding site and a chitin-binding site, which facilitated the efficient precipitation of $CaCO_3$ on the chitin matrix (Figure 1). The effect of the novel fusion protein on $CaCO_3$ crystallization and sand densification was investigated using urease-based mineralization. This study is the first to address the use of urease-based mineralization to generate organic−inorganic composite materials using a newly developed recombinant protein.

MATERIALS AND METHODS

Materials. The synthetic gene of the chitin-binding domain (ChBD) from chitinase A1 from *Bacillus circulans* WL-12 (GenBank: AAA81528.1) was purchased from Eurofins Genomics (Tokyo, Japan)

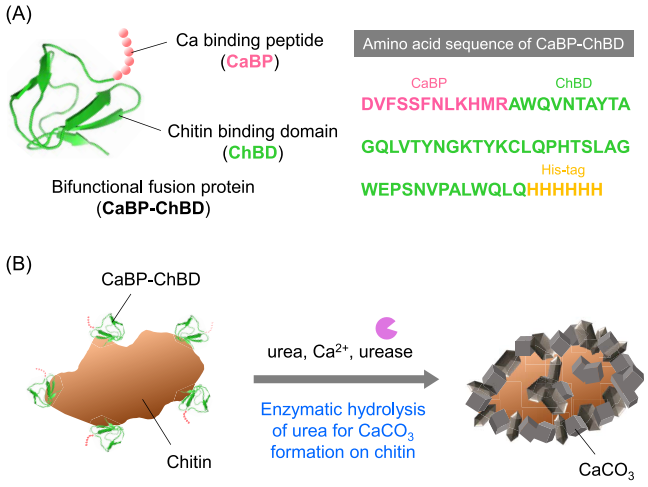

Figure 1. Structure and function of CaBP-ChBD: (A) schematic ribbon drawing and the amino acid sequence of CaBP-ChBD and (B) $CaCO_3$ formation on chitin through the fusion protein.

and optimized for expression in *Escherichia coli*. Calcite-binding peptide (CaBP: DVFSSFNLKHMR) derived from the phage-display system[33,34] was purchased from Gen Script (Tokyo, Japan). Tryptone and yeast extract were purchased from BD Biosciences Advanced Bioprocessing (Miami, FL). Ampicillin and isopropyl β-D-1thiogalactopyranoside (IPTG) were obtained from Nacalai Tesque (Tokyo, Japan). Chitin powder was purchased from Wako Pure Chemical Industries Ltd. (Tokyo, Japan). All other organic materials and chemical reagents were purchased from Wako Pure Chemical Industries Ltd.

Gene Construction and Protein Expression. The amino acid sequence of the fusion protein (CaBP-ChBD) in this work is shown in Figure 1A. The gene encoding the fusion protein was constructed using a forward primer (AAGGAGATATACATATGGATGTGTTTAGCTCGTTCAACCTGAAACATATGCGCAAGCTTGCCTGGCAAGTCAACACTGCG) containing the CaBP gene to introduce CaBP at the N-terminal region of ChBD. The target gene for CaBP-ChBD was amplified by a polymerase chain reaction (PCR) using Prime Star Max DNA polymerase (Takara Bio, Japan) using a primer set of the forward primer described above and a reverse primer (GGTGGTGGTGCTCGAGCTGCAGCTGCCACAACGCTG). The amplified CaBP-ChBD gene was inserted into the pET-22b(+) vector, which was linearized using *Xho* I and *Nde* I restriction enzymes (New England Biolabs, Japan) using the In-Fusion system (Takara Bio) to obtain the expression vector pET-CaBP-ChBD. Here, restriction enzyme sites were selected to incorporate a His-tag at the C-terminus of CaBP-ChBD. *E. coli* DH5α was transformed with pET-CaBP-ChBD and grown in LB-Amp medium (5 mL) for 16 h at 37 °C and 160 rpm. The plasmid was extracted and subjected to DNA sequencing (Eurofins Genomics).

Escherichia coli BL21 (DE3) transformed with pET-CaBP-ChBD was cultured at 37 °C and 160 rpm until the OD_{600} reached 0.5. Then, protein expression was induced by adding 0.5 mM IPTG and shaking at 30 °C and 160 rpm for 24 h. Cells were harvested by centrifugation of the cell suspension (8000*g*, 4 °C, 10 min) and resuspended in lysis buffer. Cells were disrupted by ultrasonication (VCX-130, Sonics & Materials Inc.; strength: 30%, 2 min), and the cell lysate was centrifuged (4 °C, 12 000*g*, 20 min) to remove cell debris. The supernatant was subjected to His-tag purification using Bio-Scale Mini Nuvia IMAC Cartridges (Bio-rad Laboratories, Inc., Tokyo, Japan) because the protein was expressed as a soluble protein, which was confirmed by SDS-PAGE (Atto Company Limited, Tokyo, Japan). The purified protein was concentrated using Amicon Ultra-4 (3 kDa), and then the buffer was replaced with Tris-HCl (pH 9). Unmodified ChBD was prepared similarly to CaBP-ChBD except for using a forward primer (AAGGAGATATACATATGGCCTGGCAAGTCAACACT) that does not contain the CaBP gene.

https://doi.org/10.1021/acssuschemeng.1c03730
ACS Sustainable Chem. Eng. 2021, 9, 11493−11502

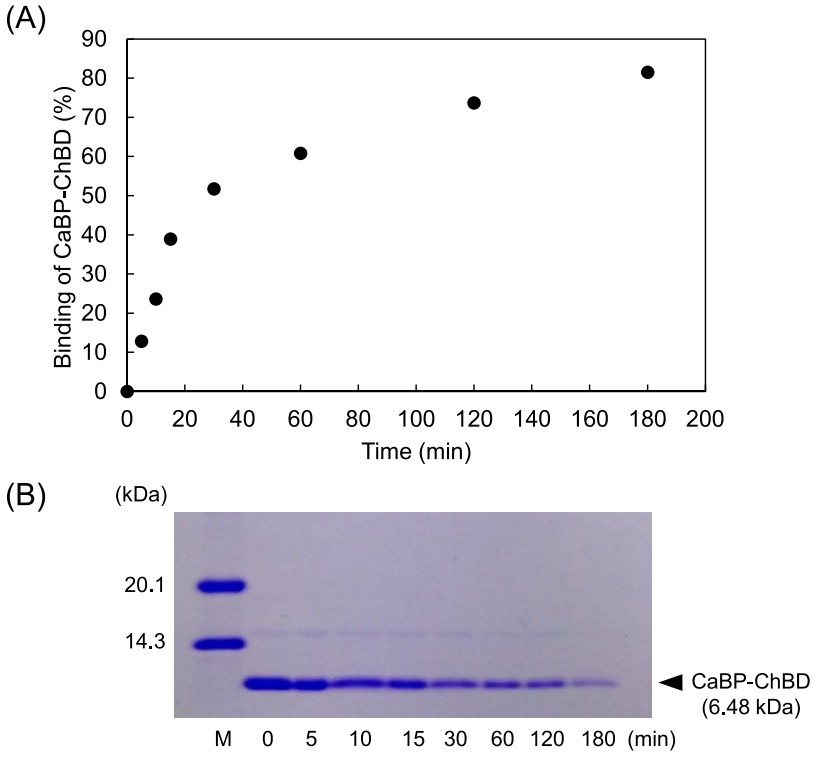

Figure 2. Binding assay of CaBP-ChBD on chitin particles evaluated by (A) the protein concentration in the supernatant by Bradford assay and (B) SDS-PAGE.

Solid-Binding Assay. The chitin-binding ability of CaBP-ChBD was studied. Chitin powder (10 mg) was mixed with CaBP-ChBD (1 ml, 0.04 mM) in 50 mM Tris-HCl buffer (pH 9) and shaken at 25 °C. Samples were collected at different time intervals (0, 5, 10, 15, 30, 60, 120, 180 min), followed by centrifugation (13 000*g*, 10 min). The protein concentration of the supernatant was measured using the Bradford method to calculate the adsorption of CaBP-ChBD on chitin. Moreover, the supernatant was analyzed by SDS-PAGE to detect the protein.

The binding ability of CaBP-ChBD (1 mL, 0.04 mM) to $CaCO_3$ in 50 mM Tris-HCl buffer (pH 9) was analyzed using a commercial $CaCO_3$ powder (purity 99.5%; Wako Pure Chemical Industries Ltd., Tokyo, Japan) in a similar manner to the procedure described above.

Effect of Additives on Urease-Catalyzed $CaCO_3$ Precipitation. $CaCO_3$ precipitation experiments were conducted by hydrolysis of urea by extracted jack bean urease (2.5 U/mL, Wako Pure Chemical Industries Ltd., Tokyo, Japan) in the presence of 0.75 mol/L of $CaCl_2$ and 0.75 mol/L of urea. Urease can hydrolyze urea to produce ammonia and bicarbonate ions. Bicarbonate ions instantaneously give $CaCO_3$ in the presence of calcium ions under alkaline conditions, which are induced by the generated ammonia.[27,28] Experiments were conducted without any peptides/proteins, with ChBD (75 μg/mL), with CaBP (75 μg/mL), with the combination of ChBD (75 μg/mL) and CaBP (75 μg/mL), with fusion protein CaBP-ChBD (75 μg/mL). All experiments were conducted with or without chitin (2.5 mg/mL).

The reaction mixture was shaken at 25 °C and 160 rpm for 24 h, followed by centrifugation (24 °C, 14 200*g*, 10 min) to separate the precipitate and supernatant. The dry weights of the precipitates were measured after oven drying at 90 °C for 24 h. The effect of bovine serum albumin (BSA; 75 μg/mL) on the $CaCO_3$ precipitation with or without chitin (2.5 mg/mL) was also investigated.

Deposition of $CaCO_3$ on Chitin. Calcium carbonate deposition on chitin mediated by CaBP-ChBD was conducted. First, CaBP-ChBD (75 μg/mL) was mixed with chitin (2.5 mg/mL) at pH 9 for 24 h to achieve adsorption equilibrium. Subsequently, EICP reaction was conducted similarly as described in the previous section. The same $CaCO_3$ formation reactions were also performed without any additives, with only CaBP-ChBD (75 μg/mL), with only chitin (2.5 mg/mL). After $CaCO_3$ formation, the precipitates were washed twice with 15 mL of distilled water, followed by lyophilization for 24 h for analysis. After coating the materials using a carbon coater (EC-32010C, JEOL, Japan), the morphology of the materials was analyzed using scanning electron microscopy (SEM; JSM-IT200 InTouchScope, JEOL, Japan) equipped with energy-dispersive X-ray spectroscopy (EDS). X-ray diffraction pattern was recorded using MultiFlex (Rigaku Co., Ltd., Tokyo, Japan; analysis condition: 40 kV, 40 mA, 2.0°/min) to identify the polymorphs of the precipitated $CaCO_3$.

Sand Solidification by EICP and MICP. Enzyme-catalyzed $CaCO_3$ formation on silica sand was conducted without additives (control), with CaBP-ChBD, with chitin, and with both chitin and CaBP-ChBD. Oven-dried (110 °C for 2 days) Mikawa silica sand (14.5 g, mean diameter D_{50} = 0.6 mm, 97.65% SiO_2) was placed in a 10 mL syringe with three layers and each layer was tamped down by a hammer 20 times. Cementation solution (0.75 M urea, 0.75 M $CaCl_2$, 10 mL) supplemented with urease (2.5 U/mL) was injected into the syringe, and then drained out from the outlet to keep the solution at 2 mm above the surface of the sand. To examine the effect of additives on solidification, CaBP-ChBD (75 μg/mL), chitin (0.145 g), or both CaBP-ChBD (75 μg/mL) and chitin (0.145 g) was introduced in sand solidification. In the case of addition of both CaBP-ChBD and chitin, CaBP-ChBD was first mixed with chitin at pH 9 for 24 h to achieve adsorption equilibrium before mixing with sand. Experiments were done in an incubator at 25 °C for 7 days. After 7 days, the samples were removed from the syringe by cutting and analyzed by SEM to understand the behavior of the CaBP-ChBD and chitin on the solidification of silica sand.

Furthermore, sand solidification was done by microbial-induced carbonate precipitation (MICP), where urease-producing bacteria *Pararhodobacter* sp. SO1[35,36] was used. Bacterial culture was prepared as previously described.[37] Oven-dried Mikawa silica sand (43.5 g) was placed in a 30 mL syringe in three layers (14.5 g each), and 20 hammer blows were given to each layer. Bacteria suspension (16 mL, OD_{600} = 1) was injected into the syringe and kept for 20 min for better fixation of the bacteria into the sand particles, followed by draining out of the solution from the outlet, leaving the solution at 2 mm above the surface

https://doi.org/10.1021/acssuschemeng.1c03730
ACS Sustainable Chem. Eng. 2021, 9, 11493−11502

of the sand. Then, cementation solution (20 mL; 0.3 M urea, 0.3 M $CaCl_2$, 3 g/L nutrient broth (BD Biosciences Advanced Bioprocessing, Miami, FL)) was added to the syringe. Then, the solution was drained out from the outlet keeping 2 mL of the solution above the surface to maintain the sand under immersed condition. Experiments were conducted in an incubator at 30 °C for 14 days. Bacteria solution (16 mL) was injected again on the seventh day. Similar experiments were conducted by adding CaBP-ChBD (75 μg/mL), chitin (0.435 g), and both chitin and CaBP-ChBD. In the case of addition of both CaBP-ChBD and chitin, CaBP-ChBD was adsorbed on chitin to reach adsorption equilibrium before mixing with sand. After 14 days, samples were removed from the syringe by cutting. Uniaxial compressive strength (UCS) and the fracture strain of the cemented samples were obtained using a uniaxial compressive machine (INSTRON 5500R; an Instron loading frame, screw-type, capacity: 250 kN) with a loading speed of 0.036 mm/min.

RESULTS AND DISCUSSION

Gene Construction and Protein Expression. Expression vectors containing the target genes (CaBP-ChBD, ChBD) were successfully constructed and confirmed by DNA sequencing. The target proteins were expressed successfully as soluble proteins in *E. coli* according to the SDS-PAGE analysis, as shown in Figure S1. Generally, lower temperatures were more favorable for IPTG to induce protein expression and to prevent the misfolding of proteins and the formation of inclusion bodies. However, CaBP-ChBD and ChBD were not expressed at lower temperatures around 15 °C; they were successfully expressed at ambient temperature (30 °C). Favorable expression temperature depends on the type of protein, and most chitin-binding proteins are expressed at ambient temperature.[32,38] The expressed proteins were successfully purified using an IMAC Ni-charged column and eluted with a high concentration of imidazole, as shown in Figure S2. The purified proteins were concentrated by ultrafiltration, and the buffer was completely replaced with Tris-HCl buffer (pH 9) because ChBD from chitinase A1 has a higher binding affinity to chitin at higher pH.[30]

Solid-Binding Assay. The binding ability of CaBP-ChBD to chitin was evaluated by incubating the protein with insoluble chitin. As shown in Figure 2A, 80% of the CaBP-ChBD was adsorbed on insoluble chitin within 3 h. The SDS-PAGE shown in Figure 2B confirmed the ability of CaBP-ChBD to adsorb on insoluble chitin. The obtained results are consistent with previous observations for the binding assay of ChBD from chitinase A1 on colloidal chitin.[30] Because the isoelectric point (pI) of the CaBP-ChBD was around 8.9, the net charge of the protein at pH 9 was almost zero. Chitin shows hydrophobic nature because of the acetyl group[39] and glucopyranose ring in *N*-acetylglucosamine unit of chitin. Hence, the hydrophobic interaction between the protein and chitin polymer chain would be a dominant factor in adsorption.

Similarly, the binding ability of CaBP-ChBD on $CaCO_3$ was evaluated by incubating the protein with $CaCO_3$ powder. The CaBP-ChBD was not efficiently adsorbed on $CaCO_3$, and only 30% of the protein was adsorbed after 24 h compared with the initial (0 h) protein concentration. Although CaBP itself has a high affinity for $CaCO_3$,[33,34] the binding ability would significantly decline when CaBP (1.5 kDa) is fused with ChBD (5 kDa), probably because of steric hindrance by the protein.

Effect of Additives on Urease-Catalyzed $CaCO_3$ Precipitation. Urease can hydrolyze urea and produce $CaCO_3$ in the presence of calcium ions (Ca^{2+}).[27,28] $CaCO_3$ precipitation was conducted by urease under various experimental conditions. The amount of $CaCO_3$ precipitates in the presence of proteins with or without chitin are shown in Figure 3. With no additive (no protein, without chitin), the amount of

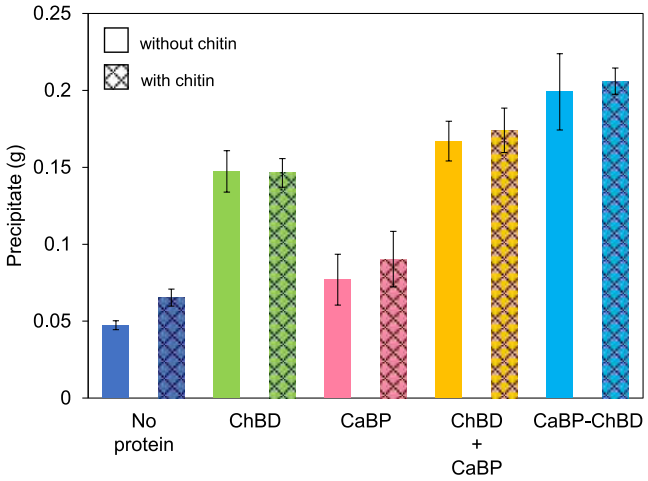

Figure 3. Amount of $CaCO_3$ precipitate in the presence of proteins with or without chitin.

precipitate was about 0.05 g, which can be estimated to 16% conversion considering that the maximum amount of $CaCO_3$ is 0.3 g in complete reaction (100% conversion). In the presence of proteins, the amount of precipitate increased drastically. The increase was more significant in the presence of ChBD moiety, where the conversion was 49% for ChBD, 56% for ChBD + CaBP, and reached to 66% for CaBP-ChBD. On the other hand, a small increment of the precipitate was obtained by adding chitin compared to that without chitin.

$CaCO_3$ formation in the presence of proteins is mostly related to the amino acid sequence of the protein. Amino acids can act as nucleation and growth-promoting molecules by reducing the activation energy of nucleation and promoting the growth of the crystals.[40] Generally, most of the proteins that facilitate $CaCO_3$ biomineralization are rich in acidic amino acids.[9,16] In contrast, few studies have revealed that acidic amino acids inhibit $CaCO_3$ crystallization and promote the stabilization of the unstable phase of $CaCO_3$.[28,41] Also, some matrix proteins that facilitate $CaCO_3$ biomineralization are rich in basic amino acid residues.[42] In our previous studies, we found that positively charged polypeptides and polysaccharides also have the ability to increase $CaCO_3$ formation.[37,43]

The CaBP used in this study was not rich in acidic amino acids, and only one aspartic acid residue was present.[33] However, it was rich in basic amino acids and contained lysine, histidine, and arginine residues. The pH of the reaction mixture was 9, and at this pH, arginine was completely positively charged, lysine was partially charged, and histidine was almost electroneutral because the dissociation constants (pK_a) of histidine, lysine, and arginine are 7, 9, and 11, respectively.[44] However, at pH 9, the carboxylic group of the aspartic acid is mostly negatively charged. Hence, CaBP can be classified as a basic peptide with a positive charge.[34]

The amino acid sequence of the ChBD was rich in basic amino acids and poor with acidic amino acids. It contained two lysines, one histidine, and one glutamic residue. The presence of the higher amounts of basic amino acid residues in both CaBP and

https://doi.org/10.1021/acssuschemeng.1c03730
ACS Sustainable Chem. Eng. 2021, 9, 11493−11502

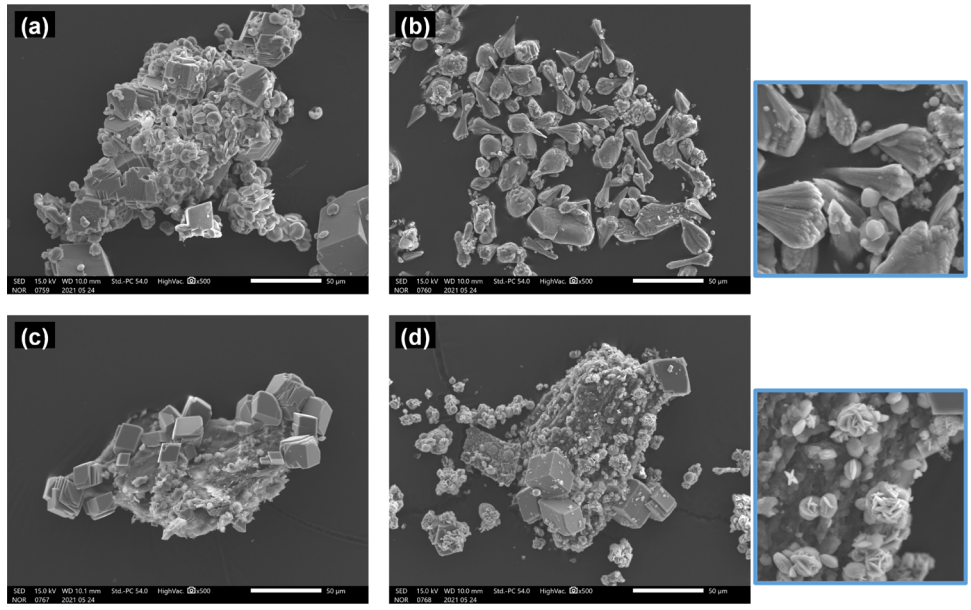

Figure 4. SEM images of the $CaCO_3$ precipitate: (a) none (control), (b) with CaBP-ChBD, (c) with chitin, and (d) with CaBP-ChBD and chitin. Images with a blue frame indicate the magnified views of (b) and (d).

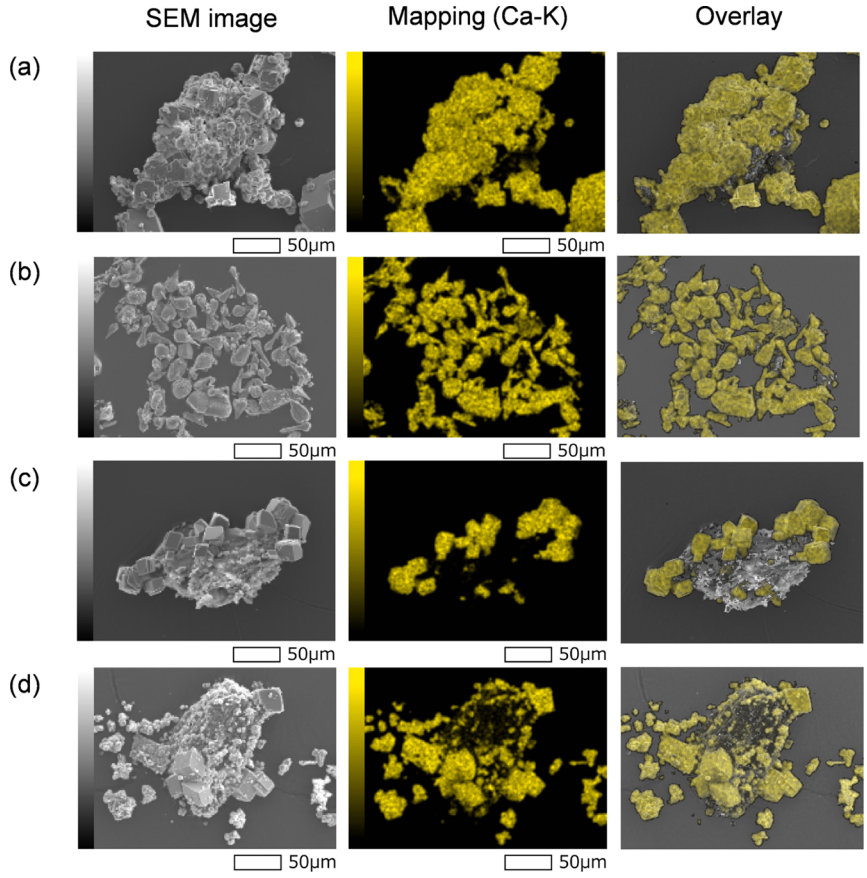

Figure 5. EDS analysis of the $CaCO_3$ precipitate: (a) none (control), (b) with CaBP-ChBD, (c) with chitin, and (d) with CaBP-ChBD and chitin.

ChBD would be the most reasonable reason for the good performance of the CaBP-ChBD in terms of $CaCO_3$ formation.

Not only the charged amino acids but also some of the amino acids with uncharged polar side chains had a considerable influence on the $CaCO_3$ crystallization. CaBP-ChBD contained cysteine, serine, and asparagine residues, which had a considerable influence on the $CaCO_3$ crystallization. In nature, cysteine-rich mineral-associated proteins can be found in lustrin A,[45] in the nacre of abalone and perlwapin.[46]

As shown in Figure 3, CaBP alone did not contribute significantly to $CaCO_3$ formation. Therefore, associated ChBD would have a considerable influence on the formation of $CaCO_3$.

https://doi.org/10.1021/acssuschemeng.1c03730
ACS Sustainable Chem. Eng. 2021, 9, 11493−11502

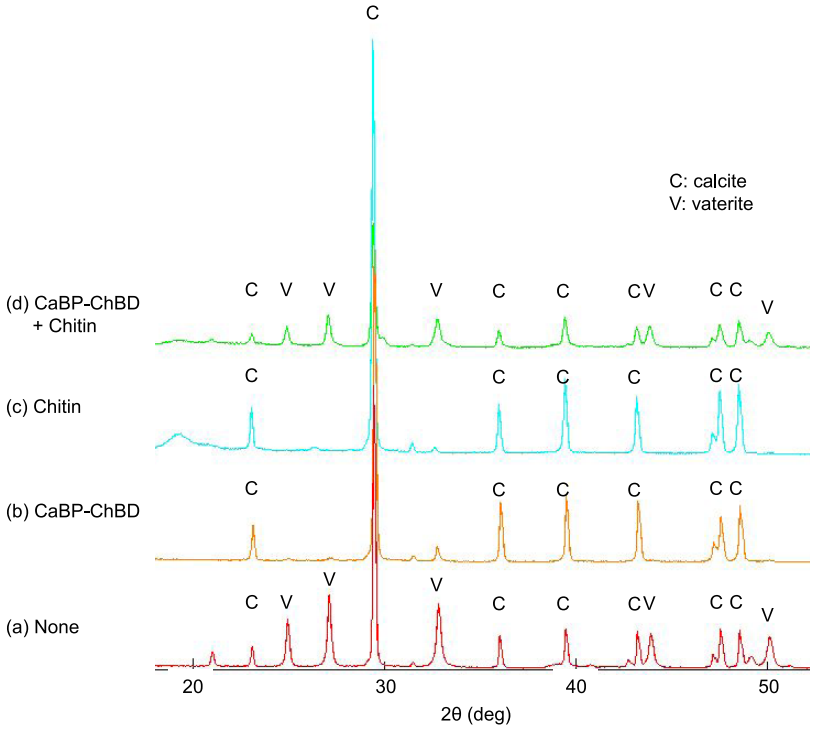

Figure 6. XRD patterns of the $CaCO_3$ precipitate: (a) none (control), (b) with CaBP-ChBD, (c) with chitin, and (d) with CaBP-ChBD and chitin.

Instead of the CaBP-ChBD, ChBD itself could increase the $CaCO_3$ formation. It is difficult to give an exact reason for this behavior of the ChBD. However, chitin and chitin-binding proteins are mainly associated with $CaCO_3$ biomineralization. In the exoskeleton of the crustacean[47] and the nacre of mollusk shells,[12] $CaCO_3$ is deposited on the chitin matrix, and this chitin matrix contributes significantly to the morphology and polymorphism of the crystals. Also, in the exoskeleton of crayfish, $CaCO_3$ is deposited upon the chitin matrix with the help of an acidic peptide containing a chitin-binding domain.[16] Therefore, ChBD would have a significant influence on $CaCO_3$ formation and morphology change, as well as its ability to bind to chitin.[18]

Another interesting point is that adding CaBP and ChBD separately did not result in better performance as did CaBP-ChBD. Most probably, the structure of CaBP-ChBD and its molecular arrangement had a significant influence on the $CaCO_3$ formation. Structural changes in the protein under alkaline conditions can also contribute significantly to its superior ability to form $CaCO_3$. Also, the close proximity of CaBP and ChBD may have had a considerable influence on the $CaCO_3$ formation. Further studies should be conducted to check the secondary structure of the protein to give a much better conclusion.

Deposition of $CaCO_3$ on Chitin. The morphology and the deposition of $CaCO_3$ on chitin induced by urease were analyzed using SEM. Figure 4 shows SEM images of $CaCO_3$ formed in the presence of the additives. As shown in Figure 4a, the precipitates mostly consisted of the mixture of rhombohedral and spherical crystals with no additives. According to the EDS analysis shown in Figure 5a and XRD pattern shown in Figure 6a, the precipitate is composed of vaterite and calcite crystals. Since vaterite has several morphologies and spherical shape is the most common type of morphology,[48] the spherical crystals in the precipitates could be vaterite. Supersaturation could possibly be a factor for the formation of vaterite crystals, meaning metastable state of $CaCO_3$ crystals are formed at higher supersaturation.[49]

In contrast, cauliflower-shaped $CaCO_3$ was found in the presence of CaBP-ChBD as shown in Figure 4b. According to EDS analysis (Figure 5b) and XRD pattern (Figure 6b), the precipitates mostly consisted of calcite. The formation of the cauliflower-shaped crystals would be presumably induced by the assembly of pillar-shaped crystals, which are elongated type of rhombohedral crystal to the *c*-axis direction when the crystallization takes place in the presence of low-molecular-weight additives such as CaBP-ChBD.[50] Previous research also reported that the formation of the cauliflower-shaped crystal is due to the adhering of pillar-shaped crystals,[51] which is consistent with our observation. Also, slow crystallization process is favorable for the formation of pillar-shaped calcite crystals.[51] In addition, protein aggregation is also possible in the presence of the $CaCl_2$, and adsorption of the protein aggregates to the growing crystals could make the crystals more porous and alter the morphology of the crystals.[52] Furthermore, a high nucleation density, low size distribution, and the absence of rhombohedral crystals are characteristics of an efficient nucleator.[53] All of these characteristics can be seen in CaBP-ChBD. Therefore, CaBP-ChBD can be classified as an efficient nucleator for $CaCO_3$ crystallization.

In the presence of chitin, rhombohedral crystals of $CaCO_3$ were deposited on the chitin particles as shown in Figures 4c and 5c. Previous studies also reported the formation of rhombohedral crystals upon a chitin matrix without matrix proteins.[16,32] As confirmed in the XRD results (Figure 6), the $CaCO_3$ crystals on chitin were identified as calcite. Previous work also reported that chitin has an ability to stabilize calcite crystal instead of vaterite.[54]

Figure 4d shows $CaCO_3$ precipitation in the presence of both CaBP-ChBD and chitin. Compared with the sample prepared only with chitin (Figure 4c), chitin particles were covered not only with rhombohedral crystals but also with small flower-shaped particles. Based on the EDS analysis in Figure 5d, these

https://doi.org/10.1021/acssuschemeng.1c03730
ACS Sustainable Chem. Eng. 2021, 9, 11493−11502

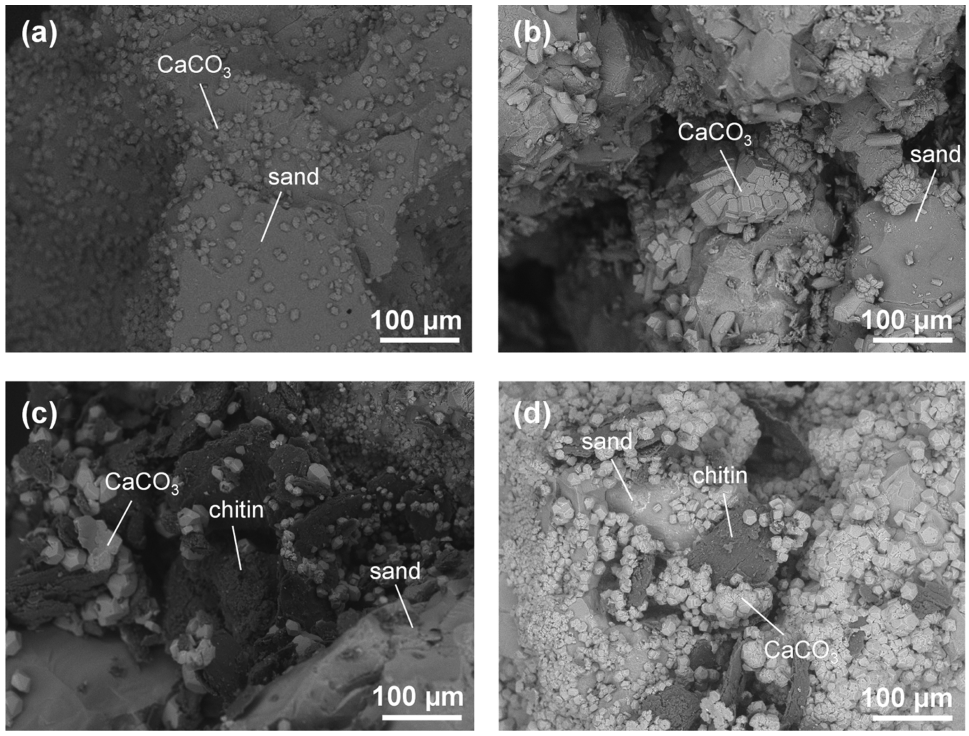

Figure 7. SEM images of solidified samples by EICP: (a) none (control), (b) with CaBP-ChBD, (c) with chitin, and (d) with CaBP-ChBD and chitin.

small particles on chitin were revealed to be $CaCO_3$. Since we could see both calcite and vaterite crystals in the precipitate according to XRD patterns in Figure 6d, the flower-shaped small particles would be vaterite while rhombohedral crystals should be calcite. Similar shape of vaterite crystal was also reported in the previous paper.[55] Density of the calcium ions on the surface of the polymer matrix is affecting greatly on the polymorphism of the $CaCO_3$ crystals. Higher calcium content on the surface of the polymer is more favorable for the stabilization of the least stable phase of the polymorphism, i.e., vaterite.[56] Accumulation of calcium ions on the chitin surface by the assistance of CaBP-ChBD might be a reason for the vaterite formation in the presence of both chitin and CaBP-ChBD. However, chitin surface was not uniformly covered with $CaCO_3$. Uniform distribution of $CaCO_3$ on the chitin could be achieved by changing the reaction rate of urea hydrolysis, which affects the deposition on chitin and the crystal size of $CaCO_3$. Changing reaction condition (with shaking or under stable condition) in EICP would be a factor in $CaCO_3$ deposition. In addition, adsorption rate of the protein into the $CaCO_3$ can be increased by reducing the crystal size. The size of the $CaCO_3$ crystals can be altered by changing the stirring time and speed and decreasing the rate of the solubilization of the salts.[57,58]

The behavior of CaBP-ChBD in terms of $CaCO_3$ formation and its morphology can be described in two ways. Fundamentally, protein can be adsorbed on chitin and chitin acts as a template for $CaCO_3$ to nucleate and grow. However, in the case of CaBP-ChBD, efficient precipitation of $CaCO_3$ on the chitin matrix occurred because of the associated CaBP, which helped to effectively form $CaCO_3$ on the chitin matrix. The protein itself contributed to the growth of $CaCO_3$ by being absorbed into the growing crystal faces.

$CaCO_3$ precipitation experiments were conducted using BSA as a control. BSA is a nonreactive protein that is abundant in plasma protein in mammals.[59] By adding BSA, small amounts (10%) of the precipitate were obtained. However, the increased amounts were not as significant as with CaBP-ChBD or other proteins. Also, the presence of uncovered chitin particles indicated that BSA did not contribute to the formation of $CaCO_3$ on the chitin matrix. Therefore, the results confirmed that the superior ability of CaBP-ChBD to form $CaCO_3$ is its unique property.

Sand Solidification by EICP and MICP. Sand solidification by enzyme-catalyzed $CaCO_3$ formation, EICP, was conducted with additives (none, CaBP-ChBD, chitin, CaBP-ChBD and chitin). We could not obtain a solidification of silica sand with no additive under the present condition and treatment time while some agglomeration of sand was found in the presence of CaBP-ChBD, chitin, and combination of CaBP-ChBD and chitin (data not shown). Figure 7 shows the SEM images of sand samples after solidification test with and without additives. Without additive (control) as shown in Figure 7a, smaller size $CaCO_3$ particles have mainly been deposited on the sand surface. Obtained results are similar to the previous observations obtained for the solidification of sand using enzyme urease.[60,61] In contrast to the control, rhombohedral $CaCO_3$ crystals and agglomeration of bigger crystals were formed on sand particles in the presence of CaBP-ChBD (Figure 7b). These crystal agglomerations would robustly form a better bridge between sand particles and led to densify the loose sand effectively. Furthermore, in addition to the crystal agglomerations, cylindrical shape crystals can be observed. The formation of cylindrical shape crystals would be due to the reassembly of the rhombohedral crystals and elongation into the *c*-axis when the crystallization takes place in the presence of low-molecular-weight additives.[53] Moreover, formation of the anisotropic shape of crystals greatly depends on the pH of the solution, where alkaline condition (pH = 9) is more favorable for the formation of anisotropic shapes such as elliptical, star-like, etc.[57] In the presence of the chitin (Figure 7c), a smaller number of

https://doi.org/10.1021/acssuschemeng.1c03730
ACS Sustainable Chem. Eng. 2021, 9, 11493−11502

polyhedron-shaped $CaCO_3$ crystals have been deposited on the chitin and sand surface. Interestingly, $CaCO_3$ formation was facilitated significantly and effectively with both CaBP-ChBD and chitin (Figure 7d). The most important point is that pore spaces between the sand particle have been filled efficiently in this system. In the sand densification process, effective filling of the pore spaces between the sand particles and the development of a bridge between the sand particles are essential to get better strength and stiffness for the sand specimen.[62]

Furthermore, sand solidification by MICP using urease-producing bacteria was conducted with the additives. MICP is a promising approach for sand solidification compared to EICP because the microbes produce appreciable amounts of urease by culturing and sometimes keep producing during solidification. In addition, possible crystal nucleation sites on the surface of microbial cells would facilitate the formation of $CaCO_3$, which can act as a cementing material in solidification. In the present work, sand solidification was conducted using ureolytic bacterium *Pararhodobacter* sp. because it exhibits a high urease activity.[63] Experiments were conducted in an incubator at 30 °C because bacteria have shown the highest urease activity at 30 °C.[63] After 14 days of curing time (Figure S3), UCS and fracture strain of the cemented sand samples were determined. The UCS value of 0.24 MPa was obtained without any additives (control). The solidified sample with chitin gave a lower strength (0.19 MPa) than the control. On the other hand, a much higher strength could be achieved in the presence of CaBP-ChBD (0.44 MPa) and the combination of CaBP-ChBD and chitin (0.49 MPa). As mentioned above, efficient $CaCO_3$ formation leads to effective filling of the pore spaces between the sand particles, resulting in increased strength of the cemented samples. In the case of addition of only chitin, undesirable void space would be made between sand particles, resulting in the lack of bonding of the particles. Optimization of the amount of chitin could improve the strength.

In terms of fracture strain, the control sample gave the value of 0.014. The lower fracture strain was observed in chitin (0.003) and in CaBP-ChBD (0.007). In CaBP-ChBD system, a higher USC value was obtained, but the material could become brittle because of the significant formation of solid $CaCO_3$ crystals. In contrast, higher fracture strain was obtained in the combination of CaBP-ChBD and chitin (0.017). The combination of CaBP-ChBD and chitin could make the solidified samples more ductile instead of brittle. The major drawback of the biocementation by MICP is brittleness of the solidified sample.[64] Therefore, the combination of CaBP-ChBD and chitin could give the best property of high strength and ductility. Further investigation is necessary for detailed evaluation of the effect of CaBP-ChBD and chitin, considering the shear behavior of solidified samples.

CONCLUSIONS

A novel recombinant protein CaBP-ChBD was developed by the fusion of ChBD with CaBP. CaBP-ChBD facilitated the formation of $CaCO_3$ on the chitin matrix. The morphology of $CaCO_3$ was significantly changed in the presence of CaBP-ChBD and chitin. In addition, the combination of CaBP-ChBD and chitin provided desirable properties in biocementation to improve the strength of loose sandy soil. The developed recombinant protein could be further modified or designed for optimization and functionalization for $CaCO_3$−organic hybrid materials, which can be used as an efficient and sustainable biocementation, as well as for other industrial applications in tissue engineering, biomedical engineering, etc.

ASSOCIATED CONTENT

Supporting Information

The Supporting Information is available free of charge at https://pubs.acs.org/doi/10.1021/acssuschemeng.1c03730.

SDS-PAGE analyses for the expression of CaBP-ChBD and ChBD, SDS-PAGE analyses for the His-tag purification of the proteins, and sand solidification by MICP with additives (PDF)

AUTHOR INFORMATION

Corresponding Author

Kazunori Nakashima − *Division of Sustainable Resources Engineering, Faculty of Engineering, Hokkaido University, Sapporo 060-8628, Japan*; orcid.org/0000-0003-4492-104X; Phone: +81-11-706-6322; Email: k.naka@eng.hokudai.ac.jp

Authors

Thiloththama H. K. Nawarathna − *Division of Sustainable Resources Engineering, Graduate School of Engineering, Hokkaido University, Sapporo 060-8628, Japan*

Tetsuya Kawabe − *Division of Sustainable Resources Engineering, Graduate School of Engineering, Hokkaido University, Sapporo 060-8628, Japan*

Wilson Mwandira − *Division of Sustainable Resources Engineering, Graduate School of Engineering, Hokkaido University, Sapporo 060-8628, Japan*

Kiyofumi Kurumisawa − *Division of Sustainable Resources Engineering, Faculty of Engineering, Hokkaido University, Sapporo 060-8628, Japan*

Satoru Kawasaki − *Division of Sustainable Resources Engineering, Faculty of Engineering, Hokkaido University, Sapporo 060-8628, Japan*

Complete contact information is available at: https://pubs.acs.org/10.1021/acssuschemeng.1c03730

Notes

The authors declare no competing financial interest.

ACKNOWLEDGMENTS

This work was partly supported by JSPS KAKENHI Grant Numbers JP18H03395 and JP21H03627. The authors thank Prof. Y. Fujii at Hokkaido University for allowing them to use uniaxial compressive machine and R. Ishikawa at Technical Center of Engineering, Hokkaido University, for her support in SEM-EDS analyses.

REFERENCES

(1) Mann, S. *Biomineralization, Principles and Concepts in Bioinorganic Materials Chemistry*; Oxford University Press: Oxford, U.K., 2001.

(2) Estroff, L. A. Biomineralization. *Chem. Rev.* **2008**, *108*, 4329−4331.

(3) Arakaki, A.; Shimizu, K.; Oda, M.; Sakamoto, T.; Nishimura, T.; Kato, T. Biomineralization-inspired Synthesis of Functional Organic/Inorganic Hybrid Materials: Organic Molecular Control of Self-Organization of Hybrids. *Org. Biomol. Chem.* **2015**, *13*, 974−989.

(4) Kumagai, H.; Matsunaga, R.; Nishimura, T.; Yamamoto, Y.; Kajiyama, S.; Oaki, Y.; Akaiwa, K.; Inoue, H.; Nagasawa, H.; Tsumoto, K.; Kato, T. $CaCO_3$/Chitin Hybrids: Recombinant Acidic Peptides Based on a Peptide Extracted from the Exoskeleton of a Crayfish Controls the Structures of the Hybrids. *Faraday Discuss.* **2012**, *159*, 483−494.

(5) Dorozhkin, S. V.; Epple, M. Biological and Medical Significance of Calcium Phosphates. *Angew. Chem., Int. Ed.* **2002**, *41*, 3130−3146.
(6) Weiner, S.; Addadi, L. Design Strategies in Mineralized Biological Materials. *J. Mater. Chem.* **1997**, *7*, 689−702.
(7) Kröger, N.; et al. Polycationic Peptides from Diatom Biosilica that Direct Silica Nanosphere Formation. *Science* **1999**, *286*, 1129−1132.
(8) Shimizu, K.; Cha, J.; Stucky, G. D.; Morse, D. E. Silicatein: Cathepsin L-like Protein in Sponge Biosilica. *Proc. Natl. Acad. Sci. U.S.A.* **1998**, *95*, 6234−6238.
(9) De Oliveira, D. B.; Laursen, R. A. Control of Calcite Crystal Morphology by a Peptide Designed to Bind to a Specific Surface. *J. Am. Chem. Soc.* **1997**, *119*, 10627−10631.
(10) Gebauer, D.; Verch, A.; Borner, H. G.; Colfen, H. Influence of Selected Artificial Peptides on Calcium Carbonate Precipitation - A Quantitative Study. *Cryst. Growth Des.* **2009**, *9*, 2398−2403.
(11) Jackson, A. P.; Vincent, J. F. V.; Turner, R. M. Comparison of Nacre with Other Ceramic Composites. *J. Mater. Sci.* **1990**, *25*, 3173−3178.
(12) Sun, J.; Bhushan, B. Hierarchical Structure and Mechanical Properties of Nacre: A Review. *RSC Adv.* **2012**, *2*, 7617−7632.
(13) Inoue, H.; Ozaki, N.; Nagasawa, H. Purification and Structural Determination of a Phosphorylated Peptide with Anti-calcification and Chitin Binding Activities in the Exoskeleton of Crayfish, Procambarus clarkii. *Biosci. Biotechnol. Biochem.* **2001**, *65*, 1840−1848.
(14) Suzuki, M.; Saruwatari, K.; Kogure, T.; Yamamoto, Y.; Nishimura, T.; Kato, T.; Nagasawa, H. An Acidic Matrix Protein, Pif, is a Key Macromolecule for Nacre Formation. *Science* **2009**, *325*, 1388−1390.
(15) Sudo, S.; Fujikawa, T.; Ohkubo, T.; Sakaguchi, K.; Tanaka, M.; Nakashima, K.; et al. Structures of Mollusc Shell Framework Proteins. *Nature* **1997**, *387*, 563−564.
(16) Sugawara, A.; Nishimura, T.; Yamamoto, Y.; Inoue, H.; Nagasawa, H.; Kato, T. Self-organization of Oriented Calcium Carbonate/Polymer Composites: Effects of a Matrix Peptide Isolated from the Exoskeleton of a Crayfish. *Angew. Chem., Int. Ed.* **2006**, *45*, 2876−2879.
(17) Rebers, J. E.; Riddiford, L. M. Structure and Expression of a *Manduca Sexta* Larval Cuticle Gene Homologous to *Drosophila* Cuticle Genes. *J. Mol. Biol.* **1988**, *203*, 411−423.
(18) Jin, C.; Zhao, J.; Pu, J.; Liu, X.; Li, J. Hichin, a Chitin Binding Protein is Essential for the Self-Assembly of Organic Frameworks and Calcium Carbonate During Shell Formation. *Int. J. Biol. Macromol.* **2019**, *135*, 745−751.
(19) Nakayamaa, S.; Suzukia, M.; Endoa, H.; Iimuraa, K.; Kinoshitac, S.; Watabec, S.; Kogureb, T.; Nagasawaa, H. Identification and Characterization of a Matrix Protein (PPP-10) in the Periostracum of the Pearl Oyster, Pinctada Fucata. *FEBS Open Bio.* **2013**, *3*, 421−427.
(20) Suzuki, M.; Iwashima, A.; Tsutsui, N.; Ohira, T.; Kogure, T.; Nagasawa, H. Identification and Characterisation of a Calcium Carbonate-Binding Protein, Blue Mussel Shell Protein (BMSP), from the Nacreous Layer. *Chem. Bio. Chem.* **2011**, *12*, 2478−2487.
(21) Montagnani, C.; Marie, B.; Marin, F.; Belliard, C.; Riquet, F.; Tayale, A.; Zanella-Cleon, I.; Fleury, E.; Gueguen, Y.; Piquemal, D.; Cochennec-Laureau, N. *Pmarg*-Pearlin is a Matrix Protein Involved in Nacre Framework Formation in the Pearl Oyster *Pinctada margaritifera*. *Chem. Bio. Chem.* **2011**, *12*, 2033−2043.
(22) Launey, M. E.; Ritchie, R. O. On the Fracture Toughness of Advanced Materials. *Adv. Mater.* **2009**, *21*, 2103−2110.
(23) Whiffin, V. S.; Van Paassen, L. A.; Harkes, M. P. Microbial Carbonate Precipitation as a Soil Improvement Technique. *Geomicrobiol. J.* **2007**, *24*, 417−423.
(24) DeJong, J. T.; Fritzges, M. B.; Nusslein, K. Microbially Induced Cementation to Control Sand Response to Undrained Shear. *J. Geotech. Geoenviron. Eng.* **2006**, *132*, 1381−1392.
(25) Gowthaman, S.; Mitsuyama, S.; Nakashima, K.; Komatsu, M.; Kawasaki, S. Biogeotechnical Approach for Slope Soil Stabilization Using Locally Isolated Bacteria and Inexpensive Low-Grade Chemicals: A Feasibility Study on Hokkaido Expressway Soil, Japan. *Soils Found.* **2019**, *59*, 484−499.
(26) Maroney, M. J.; Ciurli, S. Nonredox Nickel Enzymes. *Chem. Rev.* **2014**, *114*, 4206−4228.
(27) Hamdan, N.; Zhao, Z.; Mujica, M.; Kavazanjian, E.; He, X. Hydrogel-Assisted Enzyme-Induced Carbonate Mineral Precipitation. *J. Mater. Civ. Eng.* **2016**, *28*, No. 04016089.
(28) Zhao, Z.; Hamdan, N.; Shen, L.; Nan, H.; Almajed, A.; Kavazanjian, E.; He, X. Biomimetic Hydrogel Composites for Soil Stabilization and Contaminant Mitigation. *Environ. Sci. Technol.* **2016**, *50*, 12401−12410.
(29) Yang, T. L. Chitin-Based Materials in Tissue Engineering: Applications in Soft Tissue and Epithelial Organ. *Int. J. Mol. Sci.* **2011**, *12*, 1936−1963.
(30) Hashimoto, M.; Ikegami, T.; Seino, S.; Ohuchi, N.; Fukada, H.; Sugiyama, J.; Shirakawa, M.; Watanabe, T. Expression and Characterization of the Chitin-Binding Domain of Chitinase A1 from *Bacillus circulans* WL-12. *J. Bacteriol.* **2000**, *182*, 3045−3054.
(31) Jee, J.-G.; Ikegami, T.; Okada, T.; Hashimoto, M.; Seino, S.; Watanabe, T.; Shirakawa, M. Solution Structure of the Fibronectin Type III Domain From *Bacillus Circulans* WL-12 Chitinase A1. *J. Biol. Chem.* **2002**, *277*, 1388−1397.
(32) Ping, H.; Wan, Y.; Xie, H.; Xie, J.; Wang, W.; Wang, H.; Munir, Z. A.; Fu, Z. Organized Arrangement of Calcium Carbonate Crystals, Directed by a Rationally Designed Protein. *Cryst. Growth Des.* **2018**, *18*, 3576−3583.
(33) Gaskin, D. J. H.; Starck, K.; Vulfson, E. N. Identification of Inorganic Crystal-Specific Sequences Using Phage Display Combinatorial Library of Short Peptides: A Feasibility Study. *Biotechnol. Lett.* **2000**, *22*, 1211−1216.
(34) Sarikaya, M.; Tamerler, C.; Jen, A. K.; Schulten, K.; Baneyx, F. Molecular Biomimetics: Nanotechnology Through Biology. *Nat. Mater.* **2003**, *2*, 577−585.
(35) Danjo, T.; Kawasaki, S. Microbially Induced Sand Cementation Method Using *Pararhodobacter* sp. Strain SO1, Inspired by Beach Rock Formation Mechanism. *Mater. Trans., JIM* **2016**, *57*, 428−437.
(36) Danjo, T.; Kawasaki, S. A study of the Formation Mechanism of Beach Rock in Okinawa, Japan: Toward Making Artificial Rock. *Int. J. Geomate* **2013**, *5*, 634−639.
(37) Nawarathna, T. H. K.; Nakashima, K.; Fujita, M.; Takatsu, M.; Kawasaki, S. Effects of Cationic Polypeptide on $CaCO_3$ Crystallization and Sand Solidification by Microbial-Induced Carbonate Precipitation. *ACS Sustainable Chem. Eng.* **2018**, *6*, 10315−10322.
(38) Lobo, M. D.; Silva, F. D.; Landim, P. G.; da Cruz, P. R.; de Brito, T. L.; de Medeiros, S. C.; Oliveira, J. T.; Vasconcelos, I. M.; Pereira, H. D.; Grangeiro, T. B. Expression and Efficient Secretion of a Functional Chitinase from *Chromobacterium violaceum* in *Escherichia coli*. *BMC Biotechnol.* **2013**, *13*, No. 46.
(39) Cui, J.; Yu, Z.; Lau, D. Effect of Acetyl Group on Mechanical Properties of Chitin/Chitosan Nanocrystal: A Molecular Dynamics Study. *Int. J. Mol. Sci.* **2016**, *17*, 61−74.
(40) Briegel, C.; Seto, J. Single Amino Acids as Additives Modulating $CaCO_3$ Mineralization. In *Advanced Topics in Biomineralization*; 2012; pp 33−48.
(41) Njegic Dzakula, B.; Falini, G.; Kralj, D. Crystal Growth Mechanism of Vaterite in the Systems Containing Charged Synthetic Poly(Amino Acids). *Croat. Chem. Acta.* **2018**, *90*, 689−698.
(42) Jain, G.; Pendola, M.; Huang, Y. C.; Gebauer, D.; Evans, J. S. A Model Sea Urchin Spicule Matrix Protein, rSpSM50, is a Hydrogelator that Modifies and Organizes the Mineralization Process. *Biochemistry* **2017**, *56*, 2663−2675.
(43) Nawarathna, T. H. K.; Nakashima, K.; Kawasaki, S. Chitosan Enhances Calcium Carbonate Precipitation and Solidification Mediated by Bacteria. *Int. J. Biol. Macromol.* **2019**, *133*, 867−874.
(44) Voet, D. J.; Voet, J. G.; Pratt, C. W. *Fundamentals of Biochemistry*, 4th ed.; John Wiley & Sons: 111 River Street, Hoboken, NJ, 2013.
(45) Chen, T.; Small, D. A.; Wu, L. Q.; Rubloff, G. W.; Ghodssi, R.; Vazquez-Duhalt, R.; Bentley, W. E.; Payne, G. F. Nature-Inspired Creation of Protein-Polysaccharide Conjugate and Its Subsequent Assembly onto a Patterned Surface. *Langmuir* **2003**, *19*, 9382−9386.

https://doi.org/10.1021/acssuschemeng.1c03730
ACS Sustainable Chem. Eng. 2021, 9, 11493−11502

(46) Treccani, L.; Mann, K.; Heinemann, F.; Fritz, M. Perlwapin, an Abalone Nacre Protein with Three Four-Disulfide Core (Whey Acidic Protein) Domains, Inhibits the Growth of Calcium Carbonate Crystals. *Biophys. J.* **2006**, *91*, 2601−2608.
(47) Raabe, D.; Sachs, C.; Romano, P. The Crustacean Exoskeleton as an Example of a Structurally and Mechanically Graded Biological Nanocomposite Material. *Acta Mater.* **2005**, *53*, 4281−4292.
(48) Wu, J.; Zeng, R. J. Biomimetic Regulation of Microbially Induced Calcium Carbonate Precipitation Involving Immobilization of *Sporasarcina Pasteurii* by Sodium Alginate. *Cryst. Growth Des.* **2017**, *17*, 1854−1862.
(49) Trushina, D. B.; Bukreeva, T. V.; Kovalchuk, M. V.; Antipina, M. N. $CaCO_3$ Vaterite Microparticles for Biomedical and Personal Care Applications. *Mater. Sci. Eng.: C* **2014**, *45*, 644−658.
(50) Didymus, J. M.; Oliver, P.; Mann, S.; DeVries, A. L.; Hauschka, P. V.; Westbroek, P. Influence of Low-Molecular-Weight and Macromolecular Organic Additives on the Morphology of Calcium Carbonate. *J. Chem. Soc., Faraday Trans.* **1993**, *89*, 2891−2900.
(51) Zhang, C.; Li, F.; Lv, J. Morphology and Formation Mechanism in Precipitation of Calcite Induced by *Curvibacter lanceolatus* strain HJ-1. *J. Cryst. Growth* **2017**, *478*, 96−101.
(52) Vikulina, A. S.; Feoktistova, N. A.; Balabushevich, N. G.; Skirtachd, A. G.; Volodkinab, D. The Mechanism of Catalase Loading into Porous Vaterite $CaCO_3$ Crystals by Co-synthesis. *Phys. Chem. Chem. Phys.* **2018**, *20*, 8822−8831.
(53) Donners, J. J. J. M.; Nolte, R. J. M.; Sommerdijk, N. A. J. M. A Shape-Persistent Polymeric Crystallization Template for $CaCO_3$. *J. Am. Chem. Soc.* **2002**, *124*, 9700−9701.
(54) Hosoda, N.; Kato, T. Thin-Film Formation of Calcium Carbonate Crystals: Effects of Functional Groups of Matrix Polymers. *Chem. Mater.* **2001**, *13*, 688−693.
(55) Njegić-Džakula, B.; Falini, G.; Brecevic, L.; Skoko, Z.; Kralj, D. Effects of Initial Supersaturation on Spontaneous Precipitation of Calcium Carbonate in the Presence of Charged Poly-L-Amino Acids. *J. Colloid Interface Sci.* **2009**, *343*, 553−563.
(56) Falini, G.; Fermani, S.; Gazzano, M.; Ripamonti, A. Oriented Crystallization of Vaterite in Collagenous Matrices. *Chem.Eur. J.* **1998**, *4*, 1048−1052.
(57) Parakhonski, B. V.; Yashchenok, A. M.; Donatan, S.; Volodkin, D. V.; Tessarolo, F.; Antolini, R.; Mçhwald, H.; Skirtach, A. G. Macromolecule Loading into Spherical, Elliptical, Star-Like and Cubic Calcium Carbonate Carriers. *ChemPhysChem* **2014**, *15*, 2817−2822.
(58) Oral, C. M.; Ercan, B. Influence of pH on Morphology, Size and Polymorph of Room Temperature Synthesized Calcium Carbonate Particles. *Powder Technol.* **2018**, *339*, 781−788.
(59) Majorek, K. A.; Porebski, P. J.; Dayal, A.; Zimmerman, M. D.; Jablonska, K.; Stewart, A. J.; Chruszcz, M.; Minor, W. Structural and Immunologic Characterization of Bovine, Horse, and Rabbit Serum Albumins. *Mol. Immunol.* **2012**, *52*, 174−182.
(60) Bate, B.; Cao, J.; Zhang, C.; Hao, N. Spectral Induced Polarization Study on Enzyme Induced Carbonate Precipitations: Influences of Size and Content on Stiffness of a Fine Sand. *Acta Geotech.* **2021**, *16*, 841−857.
(61) Liu, K. W.; Jiang, N. J.; Qin, J. D.; Wang, Y. J.; Tang, C. S.; Han, X. L. An Experimental Study of Mitigating Coastal Sand Dune Erosion by Microbial- and Enzymatic-Induced Carbonate Precipitation. *Acta Geotech.* **2021**, *16*, 467−480.
(62) Harkes, M. P.; Paassen, L. A. V.; Booster, J. L.; Whiffin, V. S.; Loosdrechta, M. C. M. V. Fixation and Distribution of Bacterial Activity in Sand to Induce Carbonate Precipitation for Ground Reinforcement. *Ecol. Eng.* **2010**, *36*, 112−117.
(63) Fujita, M.; Nakashima, K.; Achal, V.; Kawasaki, S. Whole-cell Evaluation of Urease Activity of *Pararhodobacter sp*. Isolated from Peripheral Beach Rock. *Biochem. Eng. J.* **2017**, *124*, 1−5.
(64) Rahman, M. M.; Hora, R. N.; Ahenkorah, I.; Beecham, S.; Karim, Md. R.; Iqbal, A. State-of-the-Art Review of Microbial-Induced Calcite Precipitation and Its Sustainability in Engineering Applications. *Sustainability* **2020**, *12*, 6281−6322.

https://doi.org/10.1021/acssuschemeng.1c03730
ACS Sustainable Chem. Eng. 2021, 9, 11493−11502